https://doi.org/10.59893/abud.24(2).016
Acta Biol. Univ. Daugavp. 24(2) 2024
ISSN

FAST AND HIGH-RESOLUTION IMAGING OF TREMATODE MORPHOLOGICAL CHARACTERISTICS

Ilze Rubenina, Ligita Mezaraupe, Inese Gavarane, Anita Sondore, Jelena Kirilova, Sergejs Osipovs, Evita Gravele, Sanita Kecko, Veronika Pavlova, Muza Kirjusina*

Rubenina I., Mezaraupe L., Gavarane I., Sondore A., Kirilova J., Osipovs S., Gravele E., Kecko S., Pavlova V., Kirjusina M. 2024. Fast and high-resolution imaging of trematode morphological characteristics. *Acta Biol. Univ. Daugavp., 2024(2): 321-338.*

Abstract
Trematodes are parasitic flatworms, mainly have complex life cycles involving multiple hosts, including mollusks, fish, vertebrates and occasionally invertebrates. Adult trematodes have a big morphological diversity and examination of the morphological structures is important for species identification. Currently not all available tools for examination of parasite's morphology used for in depth characterization of trematode structure. Here, the authors suggest benzanthrone luminophore 3-N-pyrrolidinylbenzanthrone for fast and high-resolution imaging of morphological structures using confocal laser scanning microscopy. In this study we focused on the amphibian parasite of *Prosotocus* genus. Many species of amphibians worldwide are facing decline and have been often associated with disease. Trematode infections of amphibians can cause numerous disorders, such as grotesque limb malformations, kidney damage and debility. Applying an efficient technique for species identification and examination of morphological structures allows us to deepen understanding of co-infections, multiparasitism, host-parasite relationships, and biodiversity protection.

Keywords: *Prosotocus confusus*, trematode, morphological data, CLSM; benzanthrone dye.

*Corresponding author: *Muza Kirjusina. Department of Ecology, Institute of Life Sciences and Technologies, Daugavpils University, Parādes Str. 1A, LV-5401, Daugavpils, Latvia. E-mail: muza.kirjusina@du.lv*

Ilze Rubenina. Ligita Mezaraupe. Inese Gavarane. Jelena Kirilova. Sergejs Osipovs. Evita Gravele. Sanita Kecko. Veronika Pavlova. Department of Ecology, Institute of Life Sciences and Technologies, Daugavpils University, Parādes Str. 1A, LV-5401, Daugavpils, Latvia

Anita Sondore. Faculty of Life Sciences and Healthcare, Daugavpils University, Parādes Str. 1A, LV-5401, Daugavpils, Latvia

INTRODUCTION

Interest in the examination of trematodes has increased in the last decades and some changes can also be ascribed to increased awareness and detection. It might be also linked with an increased number of amphibian studies due to their rapid extinction. Certain trematode infections are considered to be emerging diseases of amphibians, and many can be lethal with the probability of amphibian mortality increasing with trematode load (Blaustein et al. 2012, Jayawardena et al. 2017). However, tools for trematode examination still require improvements.

Investigators rarely assess the relative importance of the detailed examination of specific morphological structures that could be considered as taxonomic keys and mainly are focused on rapid species identification. We present a novel benzanthrone luminophore for both rapid species identification and examination of morphological data. In this study, we used trematode *P. confusus*. Although there are research studies on *Prosotocus confusus Looss, 1894*, only a limited number of those studies examined the morphology and morphometry of *P. confusus* (Bursey et al. 2015, Galaktionov & Dobrovolskij 2013, Gherasim et al. 2016, Miquel et al. 2013, Skrjabin 1970). Genus *Prosotocus* contains a number of species, which are endoparasites living in the intestine of ranid frogs. *P. confusus* is a parasite of frogs *Rana ridibunda* and *R. bedriagae* (Saeed et al. 2007), *Pelophylax lessonae* (Świderski et al. 2015). *Prosotocus* flukes are one of those parasites that have evolved a biohelminthic mode of life cycle. Usually, parasite transmission can occur by ingestion of water insects infected by metacercaria (the second intermediate host), then adult trematodes mainly in frogs (the definitive host) produce eggs and in mollusks (the first intermediate host) develop cercaria that infects water insects (Gherasim et al. 2016, Poulin & Cribb 2002, Skrjabin 1970) (Fig. 1).

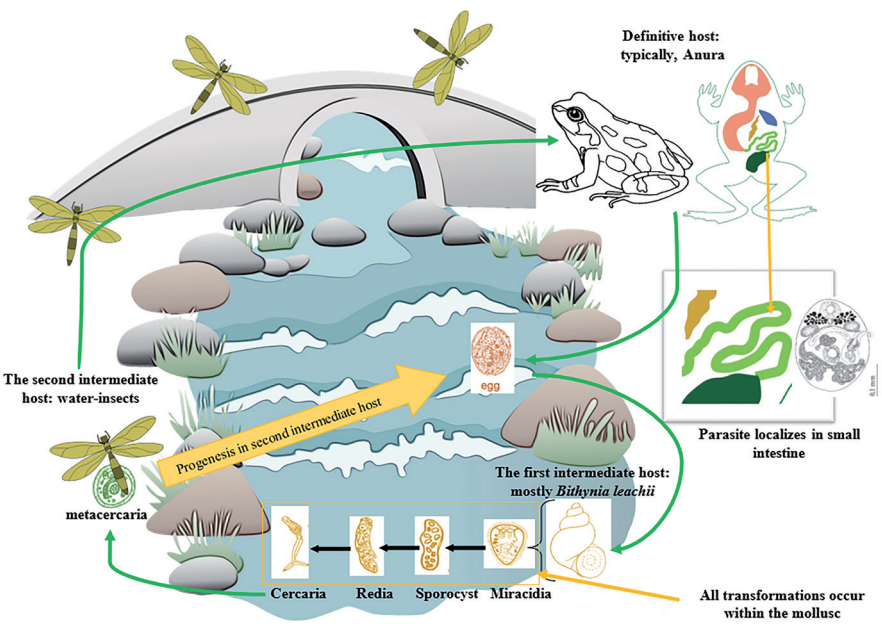

Figure 1. The life cycle of *Prosotocus confusus*. Original. Image courtesy I. Rubenina.

Morphological examination of trematodes typically involves microscopic analysis, where various staining techniques are applied to highlight different anatomical structures (Kirilova et al. 2018, Kremnev et al. 2023, Krupenko et al. 2023, Terenina et al. 2024). Techniques such as scanning electron microscopy (SEM), transmission electron microscopy (TEM) or confocal laser scanning microscopy (CLSM) are now more often used to detail the surface morphology of these parasites (Krupenko et al. 2020, Rubeniņa et al. 2021, Smirnov & Krupenko 2023). One of the interesting research objects are attachment organs, which could show us quite specific species characteristics (Krupenko & Dobrovolskij 2018). Here, we suggest a possible solution to obtain high-resolution images of trematode morphological characteristics in a short time using benzanthrone luminophore and CLSM. Work from the last several decades has identified the application of benzanthrone luminophores in biological studies (Kirilova et al. 2008, Kokina et al. 2017, Zhytniakivska et al. 2014). However, several studies indicate that benzanthrone luminophores are more appropriate for particular parasite groups and examination goals (Gavarāne et al. 2019, Gavarāne et al. 2020, Kirilova et al. 2018, Rubeniņa et al. 2021). In this work, we specifically used 3-N-pyrrolidinylbenzanthrone for fast and high-resolution imaging of trematode morphological characteristics.

MATERIAL AND METHODS

Synthesis

3-N-pyrrolidinylbenzanthrone was synthesized according to the described method (Kirilova et al. 2009).

Staining of trematodes

Adult *P. confusus* from frogs fixed in 96% ethanol (Sigma-Aldrich, Germany) were used for staining. The parasite sample was placed in luminophore 3-N-pyrrolidinylbenzanthrone for 10 min. Then the dye was washed out for three times using 96% ethanol. After the sample was placed in 96,6% ethanol (Sigma-Aldrich, Germany) – 100% xylene (VWR, United States of America) solution (1:1) for 5 min and then in 100% xylene (VWR, United States of America) for 30 seconds to obtain appropriate transparency controlled under stereomicroscope SMZ800 (Nikon, Japan). Finally, the specimens were mounted in Canada balsam (Sigma-Aldrich, United States of America) and covered with a coverslip (24x 24mm, LLG, Germany). The very last step was to dry and keep specimens in the dark until further examination under confocal laser scanning microscope. Here, we used 30 trematodes for the entire experiment.

Imaging

A confocal laser scanning microscope Eclipse Ti-E microscope equipped with a digital sight DS-U3 camera (Nikon, Japan); configured with a high-speed multiphoton A1R MP confocal laser scanning system (Nikon, Japan) was used. Images were processed by NIS Elements Advanced Research 3.2 64-bit software (Nikon, Japan). Two lasers 488 nm laser with FITC (500-550 nm) filter and 638 nm laser with a Cy5 filter (662-737 nm) were used. Slides were observed at various magnifications, from ×40 up to ×600. Autofluorescence was measured with 405 with filter 425–580 nm and 488 nm with filter 500–655 nm wavelengths, and to excite autofluorescence, equal intensities were used. The registration of the fluorescence signal was done by the internal spectral detector. The start wavelength for registration was chosen at 20 nm higher than the excitation wavelength until the edge of red visible spectra. In the optical path we didn`t use any passive cut filters. Images were acquired as Z stacks with a 2.0 µm Z step size. The morphological measurements were carried out with a computer program NIS Elements AR Analysis 3.2 64-bit.

3-N-pyrrolidinylbenzanthrone was used for imaging of various organs including attachment organs, musculature and various organ systems. New staining protocols have been developed based on previous experience with other luminophores used for biological objects (Gavarāne et al. 2019, Gavarāne et al. 2020, Kirilova et al. 2018, Kokina et al. 2017, Rubeniņa et al. 2021).

Data analysis

All analyses were performed using commercial software SPSS 24.0 for Windows (IBM Statistics).

Totally 38 morphometric measurements were carried out, 24 of which were new and not found as the trematode identification key.

There is a very large number of measurements and initially, we used the outlier exclusion criteria - Dixon's Q test for identification of outliers for each indicator (data) measured in 30 trematodes. The Dixon's Q test at a confidence level of 95% is used to only detect outliers and not to remove those, it helps with the identification of uncertainties in the data set or problems in experimental procedures. Outliers found by the test were remeasured. The indicator (data) mostly followed a normal distribution, which determined the choice of statistical analysis methods.

Descriptive statistics were used to summarize and describe continuous indicators. In this study, we provide data not only on indicators, which are usually used for species detection and classification, but also data for other important species morphological characteristics for the first time. Indicators are presented with the means as well as standard deviations in Appendix 1. We calculate 95% confidence interval which contains the true mean of the population for each indicator measured in 30 trematodes.

RESULTS

Morphological identification

Adult, live flukes were removed from small intestines of *Pelophylax esculentus* complex, *Rana temporaria* (all study specimens were sampled in Latvia) under stereomicroscope SMZ800 (Nikon, Japan) and fixed in 96% ethanol and stored at 4°C until use. The alcoholic fixative used as it fixs tissue faster than formaline-based fixatives (Rahman et al. 2022). Ethanol 96 % is less used for long term storage as it could cause tissue shrinkage and hardening (Baker 1958, Hostein et al. 2011). The samples were fixed in 96% ethanol for 3 months only as our previous studies confirmed that long-term storage can cause physical changes in a specimen (Rubeniņa et al. 2021).

Imaging

Autofluorescence image of the sample was taken before starting dying of the samples. In the autofluorescence image, no structures of the *P. confusus* but uterus with loops and vitellaria were observed. The dye used exhibits intense green luminescence and has intensive red fluorescence that allows their imaging in a spectral window that avoids sample autofluorescence. Additionally, schematic drawing based on obtained morphological data of *P. confusus* features were developed (Fig. 2).

Morphological characteristics

Measurements were based on 30 specimens fixed with 96% ethanol and then stained with 3-N-pyrrolidinylbenzanthrone: 20 specimen from *P. esculentus* complex and 10 specimen from *R. temporaria.*

In this study, 3-N-pyrrolidinylbenzanthrone was applied for the first time for staining of *P. confusus* specimen to obtain general morphological data developing fast and rapid staining protocol.

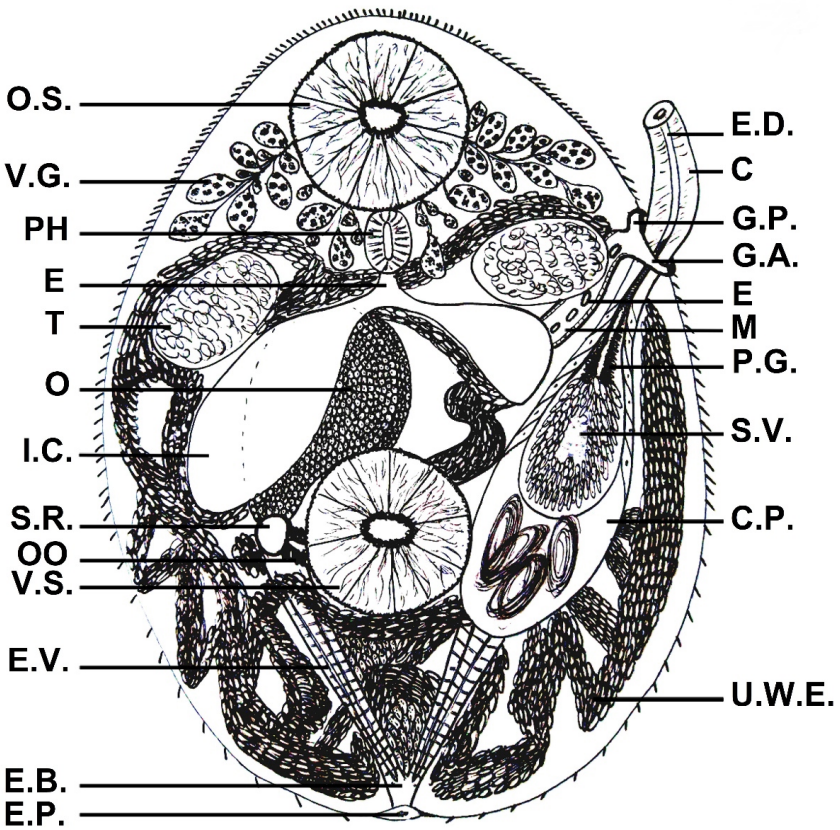

Figure 2. Schematic drawing of *P. confusus* based on obtained CLSM results. Original.
O.S. – oral sucker (acetubulum), V.G. – vitellaria glands, PH - pharynx, E – esophagus, T – testis, O – ovary, I.C. – intestinal caeca, S.R. – seminal receptacle, OO – ootype, V.S. – ventral sucker, E.V. – excretory vesicula, E.B. – excretory bladder, E.P. – excretory pore, U.W.E. – uterine filled with eggs, C.P. – copulatory organ pouch, S.V. – seminal vesicula, P.G. – prostate gland, M – metraterm, E - egg, G.A. – genital atrium, G.P. – genital pore, C – copulatory organ, E.D. – ejaculation duct. Image courtesy I. Rubenina.

Body, spikes and suckers. The body was elongated in oval with blunt anterior end and a broadly round posterior end. The average body length (+ standard deviation) was 627.70 ± 61.087 µm and body width 445.95 ± 47.968 µm accordingly. The smallest length was 493.36 µm and the largest body was 662.51 µm long. The tegument was covered with regularly arranged flattened elongated triangle-like spikes located in regular rows laying on each other (Fig. 3). We observed the spikes in the anterior part were a little wider and shorter than in the posterior end. Moreover, spikes were distributed all over the body surface, however, they were rarely distributed toward the posterior end as previously described by Skrjabin (1970). The obtained results confirmed that the surface was more densely covered in the first half of the body. The spikes were absent around the excretory pore.

The oral sucker was almost terminally located on the fore-end of the body and it was circular.

The outer surface of the oral sucker formed a fold. The average oral sucker length was 126.14 ± 14.554 µm and oral sucker width was 153.87 ± 10.689 µm. The smallest oral sucker length was 120.46 µm and maximum length was 155.36 µm. Ventral sucker was located post-equatorial and the smallest of those were 110.10 µm long while the largest sucker was 123.38 µm long.

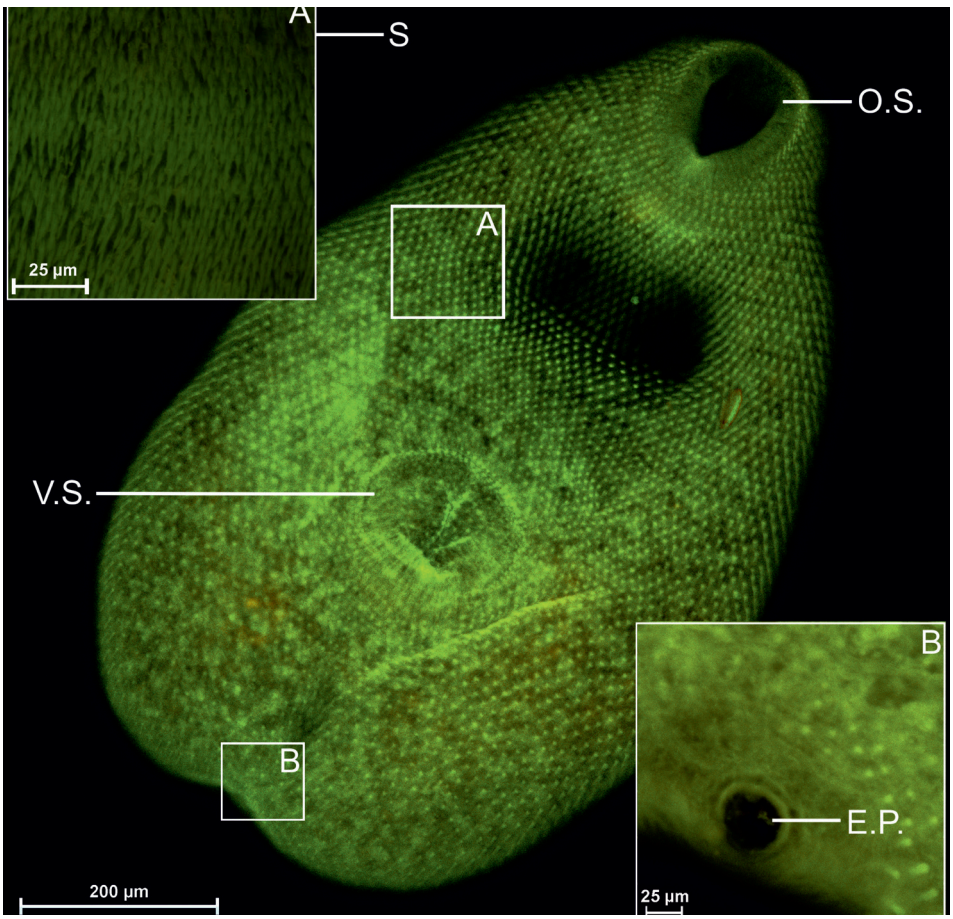

Figure 3. CLSM image of *P. confusus* surface. S – spines, O.S. – oral sucker, V.S. – ventral sucker, E.P. – excretory pore. Image courtesy L. Mezaraupe.

Musculature. The use of novel luminophore revealed all the most characteristic muscle types of Platyhelminthes such as longitudinal, diagonal and circular muscle fibers. General body muscles are made of those muscle fibers, which are located beneath the tegument. The outer circular muscle layer was identified as a thin layer of muscles running around the body of *P. confusus*. The inner longitudinal muscle layer located beneath the circular muscle and runs lengthwise along the body. Moreover, circular and longitudinal muscle fibers are closely arranged, however, circular fibers appear thicker than longitudinal muscle fibers. Transverse tegumental muscle fibers were observed. As attachment, locomotion and feeding organs are

important for internal parasites, both suckers are highly muscular. Here radial musculature predominates, however, still including circular and longitudinal muscle fibers. Looking closer into suckers it was noticed that they are more developed as there are more muscle groups to distinguish per their location – muscles covering the buccal cavity, rim and outer surface of the sucker. Muscle filaments are rarely observed as well in various parts of the digestive system, such as the intestine. Circular, longitudinal and diagonal muscle elements were observed in various parts of reproductive and excretory systems.

Digestive system. Prepharynx was observed with short length. The pharynx was globular and followed by a short esophagus. The average pharynx length was 43.99 ± 3.896 µm and width 43.79 ± 4.219 µm. The esophagus was split into two short straight digestive caeca terminated at the level of the ventral sucker in the middle third of the body. The left intestinal branch in length was shorter than intestinal right branch. Intestinal bifurcation in forebody.

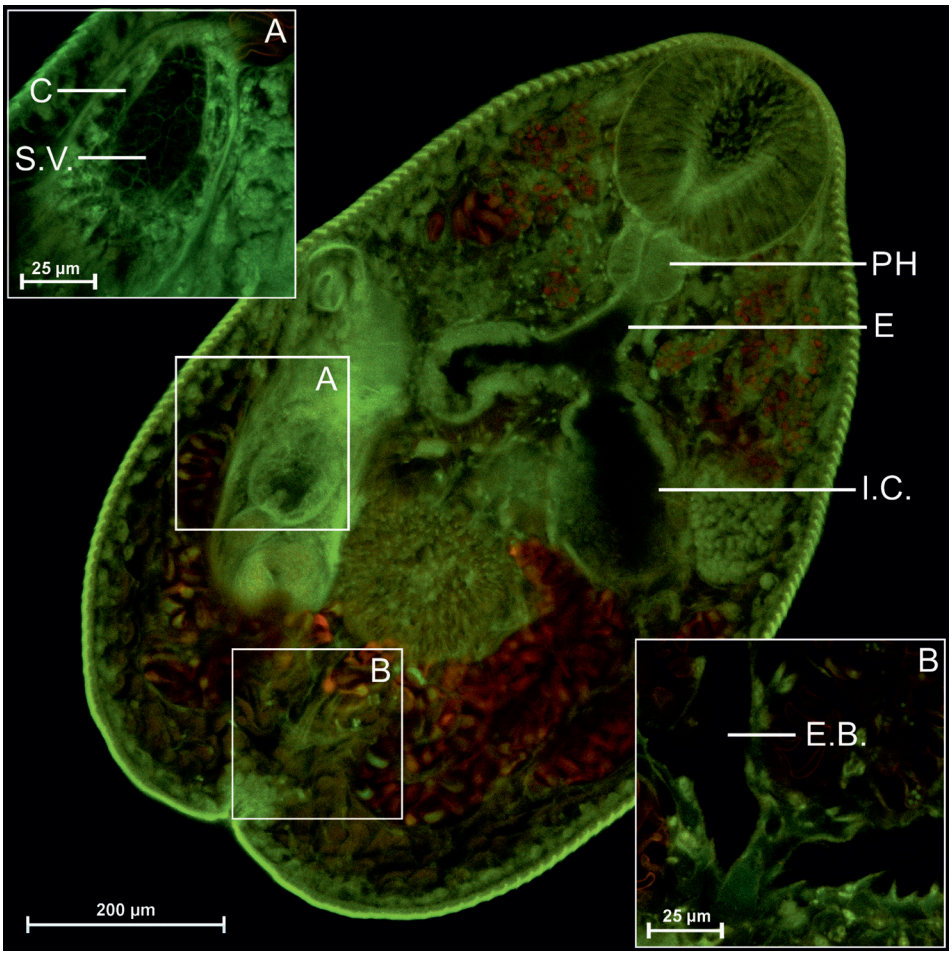

Figure 4. CLSM image of *P. confusus* digestive system and male reproductive system. PH – pharynx, E – esophagus, INT – intestine, E.B. – excretory bladder, C – cirrus, S.V. – seminal vesicle. Image courtesy L. Mezaraupe.

Reproductive system. Two large, spherical, and symmetrical testes were observed in the anterior third of the body, precaecal. The smallest testes were observed in 46.59 µm length and in 71.01 µm width while the largest in 62.22 µm length and in 84.49 µm width. Cirrus was located at left side of body. Cirrus pouch was in elongated oval form. The pouch was opening to the outside from the left side and extends anteriorly from ventral sucker zone (postequatorial). Cirrus sac contained coiled semical vesicle, pars prostatica and cirrus (Fig. 4).

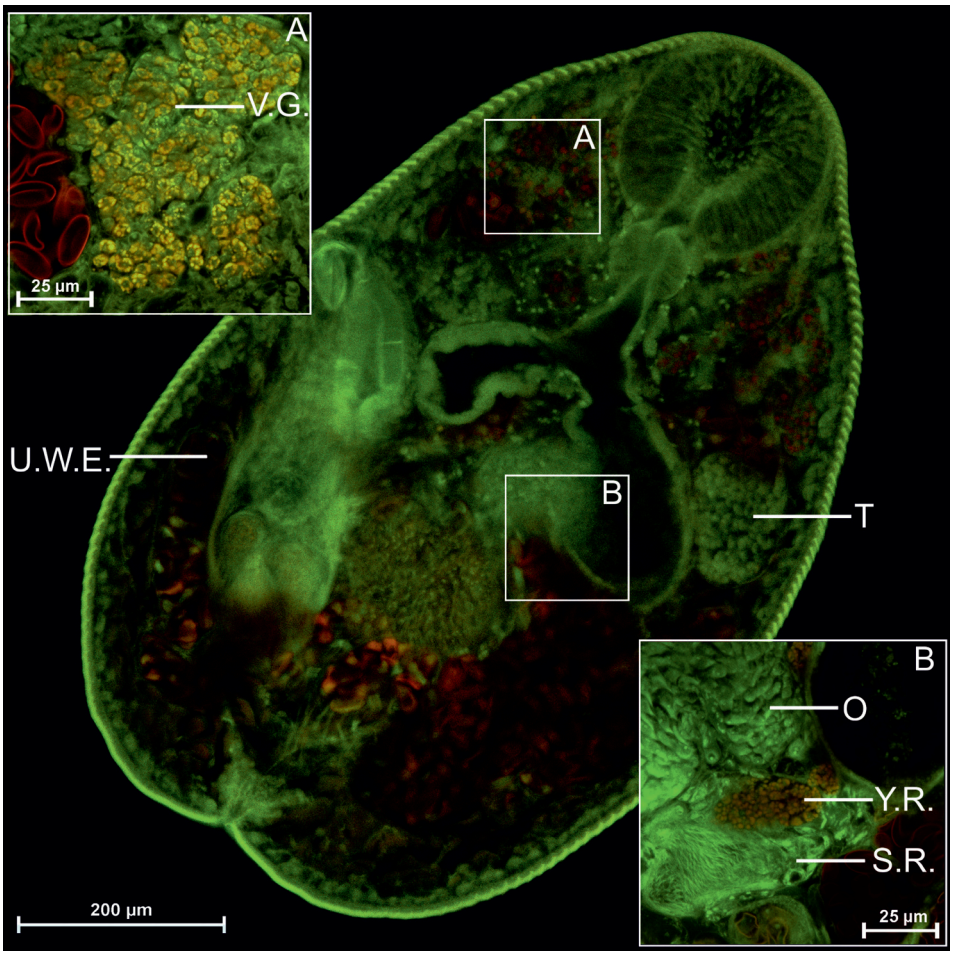

Figure 5. CLSM image of *P. confusus* female and male reproductive system. V.G. – vitellaria glands, O – ovary, Y.R. – yolk reservoir, S.R. – seminal receptacle, U.W.E. – uterus filled with eggs, T – testis. Image courtesy L. Mezaraupe.

Genital pore opened on the lateral margin of body from level of precaeca to near level of pharynx. Ovary posterior to testes and located between intestinal branches or closer to right intestinal branch. The maximum ovary length was 182.21 µm and 177.73 µm width. Uterus was long, filled most of hindbody and also may extends into forebody. It has occasional loops from the level of testes to a level of excretory pore. Metraterm was present. Uterus was filled with numerous spherical eggs. Eggs were biconcave in shape similar to erythrocyte.

The eggs have small cap called operculum. It was observed that in the level of ventral sucker coiled uterus contained eggs with four brightly visualized points (Fig. 5). Vitellaria was located in anterior part of body, bilateral extending from the mid part of oral sucker to anterior border of testes. Ootype protrude from the uterus to the right and extends to the left side of the body forming loops aimed at atrium.

DISCUSSION

Parasite species identification is crucial for life cycle description, determination of prevalence and intensity, biogeographical distribution and for interaction among species (Bajanov 1975, EL-Shabasy et al. 2024). Nowadays, CLSM is widely used for the investigation of muscular arrangement (Krupenko 2014, Marques et al. 2016, Terenina et al. 2022), parasite's internal and external structure (Kirilova et al. 2018, Kreshchenko et al. 2024) or to examine general morphology of parasite's specific attachment organs such as oral suckers (Krupenko 2019). The general parasite morphology was visualized using the luminophore 3-N-pyrrolidinyl-benzanthrone and the morphological parameters were measured. Our obtained morphometric parameters of the species *P. confusus* differed from Gherasim et al. (2016) morphometric parameters. Please refer to the Appendix 1. Length and width of body and ventral sucker parameters were similar. However, morphometric parameters for male and female reproductive systems were quite different. The root cause of differences is based when measurements have been taken. In current study, measurements done while samples were observed under confocal laser scanning microscopy. Previously Popovič and Mikeš (1989) reported the parasite's surface was covered with tiny pricks. Gherasim et al. (2016) observed that spikes were located in regular rows laying on each other and were more densely arranged toward the anterior end. In the study it was observed that left intestinal branch in length was shorter than intestinal right branch, also previously confirmed by Gherasim et al. (2016). The present study results confirmed the same – left branch is shorten than right one. The study results confirmed the same arrangement of reproductive system as was described by Lotz & Font (2008). Although, Skrjabin (1970) described that ovary was located anterior to ventral sucker or in ventral sucker zone, in our trematode samples ovary located in level of caeca in second part of body, entire or irregular. We suggested that the bright points in eggs were germinal cells based on Janardanan & Prasadan (1991) described life cycle of other trematodes where they described that miracidia has four large, uninucleated germinal cells in the posterior half of body. Excretory vesicle V-shaped and it extended to ventral sucker zone as previously described by Lotz & Font (2008) and Skrjabin (1970). The present form a little differed from those described by other authors (Lotz & Font 2008, Mashaii et al. 2000, Popovič & Mikeš 1989, Skrjabin 1970): (i) spikes are absent in region around excretory pore; (ii) ovary located in level of caeca in middle third of body. Krupenko (2014, 2019) studies showed that muscle arrangements in trematode might be very complex, therefore, various fluorescent dyes, histological sections, light and confocal laser scanning microscopy are required to visualized general morphology of the parasites. The current study and studies in literature (EL-Shabasy et al. 2024, Glagoleva et al. 2019, Kremnev et al. 2021, Kreshchenko et al. 2024, Krupenko & Dobrovolskij 2018, Terenina et al. 2022) have confirmed that trematode muscular system is quite complex and more developed in attachment organs.

CONCLUSIONS

However, during our previous studies (Gavarane et al. 2018, Gavarāne et al. 2019, Kirilova et al. 2018) performing several

experiments, it was observed that luminescent properties of the same benzanthrone dye may differ for the variable samples. Thus, not all benzanthrone luminophores are equal for simple and rapid imagining due to specific intermolecular interactiosn between the applied dye molecules and the stained object. The present study revealed that usage of CLSM and lumiphore 3-N-pyrrolidinylbenzanthrone is applicable for detailed imagining of morphological characteristics of *P. confusus*.

ACKNOWLEDGEMENTS

This work is supported by Fundamental and applied research projects of the Latvian Council of Science. Project No. lzp-2022/1-0436 "Novel fluorescent anthrone-derived functional materials for bioimaging applications". I.G. and M.K. provided the main ideas and wrote the manuscript; A.S. carried out statistics; E.G. provided fixed parasites for this study; J.K. and S.O. synthesis of the luminophore, measured luminescent properties and analyzed data; I.R., L.M., S.K., V.P. stained, took images and analyzed data.

REFERENCES

Bajanov M.G. 1975. O prognoze trematodi Prosotocos confusus (Loss, 1894). (On the progenesis of the trematode *Prosotocus confusus* (Looss, 1894)). *Parasitologia* 9(2): 122–126. (In Russian).

Baker J.R. 1958. Principles of Biological microtechnique: A study of fixation and dyeing. Methuen and Co. Ltd, London. 358 pp.

Blaustein A.R., Gervasi S.S., Johnson P.T.J., Hoverman J.T., Belden L.K., Bradley P.W., Xie, G.Y. 2012. Ecophysiology meets conservation: understanding the role of disease in amphibian population declines. *Philosophical Transactions of the Royal Society B* 367: 1688–1707. https://doi.org/10.1098/rstb.2012.0011

Bursey C.R., Rizvi A.N., Maity P. 2015. New species of *Prosotocus* (Digenea; Pleurogenidae) and other helminths in *Euphlyctis cyanophlyctis* (Anura: Dicroglossidae) from Punjab, India. *Acta Parasitol*ogica 60(3): 494–499. https://doi.org/10.1515/ap-2015-0070

EL-Shabasy E.A., Saleha M.A., Saidb A.E., Reda E.S. 2024. Evaluation of *schistosoma mansoni* nervous system using confocal-laser electron microscopy: nerve sensilla and FMRFamide whilereferring to F-actin abundance. *Egyptian Journal of Basic and Applied Science* 11(1): 281–296. https://doi.org/10.1080/2314808X.2024.2335853

Galaktionov K.V., Dobrovolskij A. 2013. The Biology and Evolution of Trematodes: An Essay on the Biology, Morphology, Life Cycles, Transmissions, and Evolution of Digenetic Trematodes. Spirnger Science & Business Media. 592 pp.

Gavarane I., Mezaraupe L., Rubenina I., Kirjusina M., Kirilova E. 2018. Staining of economically important parasitic nematodes by developed derivates of benzanthrone luminophore. In *18th International Multidisciplinary Scientific GeoConference SGEM 2018*. Pp. 581-588. Bulgaria: 51 Alexander Malinov blvd, Sofia. pp. 1712

Gavarāne I., Kirilova E., Rubeniņa I., Mežaraupe L., Osipovs S., Deksne G., Pučkins A., Kokina I., Bulanovs A., Kirjušina M. 2019. A Simple and Rapid Staining Technique for Sex Determination of *Trichinella* Larvae Parasites by Confocal Laser Scanning Microscopy. *Microscopy and Microanalysis* 25(6):1491–1497. https://doi.org/10.1017/S1431927619015046

Gavarāne I., Kirilova E., Rubeniņa I., Mežaraupe L., Osipovs S., Deksne G., Pučkins A., Kokina I., Bulanovs A., Kirjušina M. 2020. A simple and rapid staining technique for sex determination of *Trichinella* larvae parasites by confocal laser scanning microscopy. Highlights from Microscopy and Microanalysis. *Microscopy Today* 28(2): 58–59. https://doi.org/10.1017/S1551929519001378

Gherasim E., Erhan D., Cozari T., Rusu S., Munjiu O., Tălămbuță N. 2016. Description of species *Prosotocus confusus* Looss 1894 in conditions of central Codrii in Republic of Moldova. In: Sustainable use, protection of animal world and forest management in the context of climate change. Moldova. Pp. 131–132.

Glagoleva E.N., Yastrebova I.V., Yastrebov M.V. 2019. Body Wall Musculature of Five Representatives of the Order Paramphistomatida (Plathelminthes, Trematoda). *Biology Bulletin* 46(2): 168–178. https://doi.org/10.1134/s1062359019020067

Hostein I., Stock N., Soubeyran I., Marty M., De Mascarel I., Bui M., Geneste G., Petersen M.C., Coindre J.M., Macgrogan G. 2011. Nucleic acid quality preservation by an alcohol-based fixative: comparison with frozen tumors in a routine pathology setting. *Diagnostic Molecular Pathology* 20: 52–62. https://doi.org/10.1097/PDM.0b013e3181e71ba5

Jayawardena U.A., Rohr J.R., Amerasinghe P.H., Navaratne A.N., Rajakaruna R.S. 2017. Effects of agrochemicals on disease severity of *Acanthostomum burminis* infections (Digenea: Trematoda) in the Asian common toad, *Duttaphrynus melanostictus*. *BMC Zoology* 2(13): 1–10. https://doi.org/10.1186/s40850-017-0022-1

Janardanan K.P., Prasadan P.K. 1991. Studies on the life-cycle of *Pleurogenoides ovatus* Rao, 1977 (Trematoda: Pleurogenetinae). *Journal of Helminthology* 65(1): 43–50. https://doi.org/10.1017/S0022149X00010427

Kirilova E., Kecko S., Mežaraupe L., Gavarāne I., Pučkins A., Mickeviča I., Rubeniņa I., Osipovs S., Bulanovs A., Pupiņš M., Kirjušina M. 2018. Novel luminescent dyes for confocal laser scanning microscopy used in Trematode parasite diagnostics. *Acta Biochimica Polonica* 65(3): 449–454. https://doi.org/10.18388/abp.2018_2574

Kirilova E.M., Belyakov S.V., Kalnina I. 2009. Synthesis and study of N,N-substituted 3-amidinobenzanthrones. In Topics in Chemistry & Materials Science, Vayssilov G., Nikolova R. (eds.), Brighton, United Kingdom, Heron Press. Pp. 19–28.

Kirilova E.M., Kalnina I., Kirilov G.K., Meirovics I. 2008. Spectroscopic study of benzanthrone 3-N-derivatives as new hydrophobic fluorescent probes for biomolecules. *Journal of Fluorescence* 18: 645–648. https://doi.org/10.1007/s10895-008-0340-3

Kokina I., Mickeviča I., Jahundoviča I., Ogurcovs A., Krasovska M., Jermaļonoka M., Mihailova I., Tamanis E., Gerbreders V. 2017. Plant Explants Grown on Medium Supplemented with Fe 3 O 4 Nanoparticles Have a Significant Increase in Embryogenesis. *Journal of Nanomaterials* 3: 1–11. https://doi.org/10.1155/2017/4587147

Kremnev G., Gonchar A., Krapivin V., Uryadova A., Miroliubov A., Krupenko D. 2021. Life cycle truncation in Digenea, a case study of *Neophasis* spp. (Acanthocolpidae). *International Journal for Parasitology: Parasites and Wildlife* 15: 158–172. https://doi.org/10.1016/j.ijppaw.2021.05.001

Kremnev G., Gonchar A., Uryadova A., Krapivin V., Skobkina O., Gubler A., Krupenko D. 2023. No Tail No Fail: Life Cycles of the Zoogonidae (Digenea). *Diversity* 15(1): 121. https://doi.org/10.3390/d15010121

Kreshchenko N.D., Terenina N.B., Poddubnaya L.G., Voropaeva E.L., Mochalova N.V., Kuznetsov G.V., Movsesyan S.O. 2024. *Acrolichanus auriculatus* (Digenea, Allocreadiidae): distribution of sensory papillae, musculature and FMRFamide-like immunoreactivity in adult worms. *Zoomorphology* 143(2): 313–328. https://doi.org/10.1007/s00435-024-00665-4

Krupenko D. 2019. Oral sucker in Digenea: structure and muscular arrangement. *Zoomorphology* 138(1): 29–37. https://doi.org/10.1007/s00435-018-0423-x

Krupenko D., Dobrovolskij A.A. 2018. Morphological framework for attachment and locomotion in several Digenea of the families Microphallidae and Heterophyidae. *Parasitology Research* 117(12): 3799–3807. https://doi.org/10.1007/s00436-018-6085-2

Krupenko D., Miroliubov A., Kryukov E., Faure L., Minemizu R., Haag L., Lundgren M., Kameneva P., Kastriti M.E., Adameyko I. 2023. Polymorphic parasitic larvae cooperate to build swimming colonies luring hosts. *Current Biology* 33(20): 4524–4531.e4. https://doi.org/10.1016/j.cub.2023.08.090

Krupenko D.Y. 2014. Muscle system of *Diplodiscus subclavatus* (Trematoda: Paramphistomida) cercariae, pre-ovigerous, and ovigerous adults. *Parasitology Research* 113: 941–952. https://doi.org/10.1007/s00436-013-3726-3

Krupenko D.Y., Gonchar A.G., Kremnev G.A., Uryadova A.A. 2020. On the life cycle of *Hemiurus levinseni* Odhner, 1905 (Digenea: Hemiuridae). *Invertebrate Zoology* 17(3): 205–218. https://doi.org/10.15298/invertzool.17.3.01

Lotz J.M., Font W.F. 2008. Family Pleurogenidae Looss, 1899. In: Gibson, D.I., Bray, R.A., Jones, A. (eds.): Keys to the Trematoda, 3rd volume. CAB, London. Pp. 563–575.

Marques J.S., Rocha B.M., Manso P.P.A., Davila S. (2016). New insights on the morphology of a digenean parasite (Digenea: Brachylaimidae, *Brachylaima mazzantii* (Travassos, 1927)) using confocal laser scanning microscopy. *Zoosystema* 39(4): 449–462. https://doi.org/10.5252/z2017n4a1

Mashaii N., Balouch M., Moubedi I. 2000. New records about helminth parasites of the marsh frog, *Rana ridibunda ridibunda* (Anura: Ranidae) from the north of Iran. *Iranian Journal of Fisheries Science* 2(2): 77–88. http://jifro.ir/article-1-3182-en.html

Miquel J., Vilavella D., Swiderski Z., Shimalov V.V., Torres, J. 2013. Spermatological characteristics of Pleurogenidae (Digenea) inferred from the ultrastructural study of *Pleurogenes claviger, Pleurogenoides medians* and *Prosotocus confusus*. *Parasite* 20(1): 28. https://doi.org/10.1051/parasite/2013028

Popovič E., Mikeš M. 1989. Infestation of taillness amphibians of genus *Rana* by trematodes in the valley of the Tisa River (Yugoslavia). *Tiscia (Szeged)* 23: 77–85.

Poulin R., Cribb T.H. 2002. Trematode life cycles: short is sweet? *Trends in Parasitology* 18(4): 176–183. https://doi.org/10.1016/S1471-4922(02)02262-6

Rahman M.A., Sultana N., Ayman U., Bhakta S., Afrose M., Afrin M., Haque Z. 2022. Alcoholic fixation over formalin fixation: A new, safer option for morphologic and molecular analysis of tissues. *Saudi Journal of Biological Sciences* 29(1): 175–182. https://doi.org/10.1016/j.sjbs.2021.08.075

Rubeniņa I., Gavarane I., Kirilova E., Mezaraupe L., Kirjusina M. 2021. Comparison of the Benzanthrone Luminophores: They Are Not Equal for Rapid Examination of *Parafasciolopsis fasciolaemorpha* (Trematoda: Digenea) *Biomolecules* 11: 598. https://doi.org/10.3390/biom11040598

Saeed I., Al-Barwari S.E., Al-Harmni K.I. 2007. A Metazoan Parasitological Research of Some Iraqi Amphibians. *Acta Parasitologica Turcica* 31(4): 337–345. PMID: 18224630.

Skrjabin K.I. 1970. Trematodi zjivotnih I ljudjei (Trematodes of animals and humans). T. 23: Fundamentals of trematodology. Publishing House of the Academy of Sciences of the USSR. 308 pp. (In Russian).

Smirnov P.A., Krupenko D.Y. 2023. Reconstruction of *Derogenes varicus* Miracidium (Digenea: Derogenidae): First Ultrastructural Description of Spines on the Surface of Hemiurata Larvae. *Parazitologia* 57(2): 108–123. https://doi.org/10.31857/S0031184723020023

Świderski Z., Miquel J., Torres J., Conn, D.B. 2014. Ultrastructural study of the egg wall surrounding the developing miracidia of the digenean *Prosotocus confusus* (Looss, 1894) (Plagiorchiida: Pleurogenidae), with the description of a unique cocoon-like envelope. *Parasitology Research* 114(1): 185–191. https://doi.org/10.1007/s00436-014-4177-1

Terenina N., Kreshchenko N., Movsesyan S. 2022. Musculature and neurotransmitters of internal organs of trematodes (the digestive, reproductive and excretory systems). *Zoology* 150: 125986. https://doi.org/10.1016/j.zool.2021.125986

Terenina N.B., Kreshchenko N.D., Movsesyan S.O. 2024. Serotonergic elements in the nervous system of parasite of acipenserid fishes, *Acrolichanus auriculatus* (Digenea: Allocreadiidae). *Micron* 185: 103690. https://doi.org/10.1016/j.micron.2024.103690

Zhytniakivska O., Trusova V., Gorbenko G., Kirilova E., Kalnina I., Kirilov G., Kinnunen P. (2014). Newly synthesized benzanthrone derivatives as prospective fluorescent membrane probes. *Journal of Luminescence* 146: 307–313. https://doi.org/10.1016/j.jlumin.2013.10.015

Received: 30.10.2024
Accepted: 29.11.2024

Appendix 1. Descriptive statistics for each indicator measured in 30 trematodes (current study) compared to other study results.

Data from	Present study				Gherasim et al., 2016		Chikhlyaev et al., 2012		Skrjabin, 1970	
Host	*Pelophylax esculentus* complex, *Rana temporaria*				*Rana ridibunda, R. lessonae* and *R.esculenta*		*R. esculenta*		*R. arvalis, R. dalmatina, R.esculenta, R. ridibunda, R. temporara, R.tigrina, Bufo calamita, B. variabilis, B. viridis, B.vulgaris, Bombina variegata, Hyla arborea*	
Country	Latvia				Moldova		Midde Volga region (Russia)		Palearctic	
Clarification	Average for all samples ± standard deviation	Standard Error of the Mean	95% confidence interval lower values	95% confidence interval upper values						
Indicator	A ± s, µm	SE Mean, µm	95.0 % CI lower values, µm	95.0 % CI upper values, µm	Min, µm	Max, µm	Min, µm	Max, µm	Min, µm	Max, µm
Body length	627.70±61.087	11.153	605.837	649.556	396	804	696	1111	390	1800
Body width	445.95±47.968	8.758	428.780	463.110	295	638	459	652	310	1000
Oral sucker length	126.14±14.554	2.657	120.934	131.350	91	153	111	148	N/M	N/M
Oral sucker width	153.87±10.689	1.952	150.047	157.697	84	168	140	170	9	240
Pharynx length	43.99±3.896	0.711	42.596	45.384	N/M	N/M	N/M	N/M	N/M	N/M
Pharynx width	43.79±4.219	0.770	42.281	45.301	N/M	N/M	N/M	N/M	N/M	N/M
Esophagus length*	55.83±6.891	1.258	53.361	58.293	N/M	N/M	N/M	N/M	N/M	N/M
Vitellaria glands length*	116.96±5.092	0.930	115.133	118.777	N/M	N/M	N/M	N/M	N/M	N/M
Vitellaria glands width*	102.43±0.802	0.146	102.142	102.716	N/M	N/M	N/M	N/M	N/M	N/M

Data from	Present study				Gherasim et al., 2016		Chikhlyaev et al., 2012		Skrjabin, 1970	
Host	*Pelophylax esculentus* complex, *Rana temporaria*				*Rana ridibunda, R. lessonae* and *R.esculenta*		*R. esculenta*		*R. arvalis, R. dalmatina, R.esculenta, R. ridibunda, R. temporara, R.tigrina, Bufo calamita, B. variabilis, B. viridis, B.vulgaris, Bombina variegata, Hyla arborea*	
Country	Latvia				Moldova		Midde Volga region (Russia)		Palearctic	
Clarification	Average for all samples ± standard deviation	Standard Error of the Mean	95% confidence interval lower values	95% confidence interval upper values						
Indicator	A ± s, µm	SE Mean, µm	95.0 % CI lower values, µm	95.0 % CI upper values, µm	Min, µm	Max, µm	Min, µm	Max, µm	Min, µm	Max, µm
Testis length	81.470±5.5648	1.016	79.479	83.461	47	141	148	170	70	320
Testis width	58.05±6.657	1.215	55.671	60.435	33	150	112	136	50	220
Intestinal caeca length*	149.51±0.550	0.101	149.310	149.704	N/M	N/M	N/M	N/M	N/M	N/M
Intestinal caeca weight*	74.55±0.365	0.067	74.417	74.678	N/M	N/M	N/M	N/M	N/M	N/M
Ovary length	162.44±31.869	5.819	151.039	173.848	42	131	140	163	100	240
Ovary width	159.69±31.420	5.736	148.442	170.928	34	171	114	131	90	260
Ventral sucker length	118.94±4.074	0.744	117.478	120.394	87	177	126	152	N/M	N/M
Ventral sucker width	116.04±5.305	0.969	114.146	117.943	91	168	133	163	9 (the same as for oral sucker)	240 (the same as for oral sucker)

Data from	Present study				Gherasim et al., 2016		Chikhlyaev et al., 2012		Skrjabin, 1970	
Host	*Pelophylax esculentus* complex, *Rana temporaria*				*Rana ridibunda, R. lessonae* and *R.esculenta*		*R. esculenta*		*R. arvalis, R. dalmatina, R.esculenta, R. ridibunda, R. temporara, R.tigrina, Bufo calamita, B. variabilis, B. viridis, B.vulgaris, Bombina variegata, Hyla arborea*	
Country	Latvia				Moldova		Midde Volga region (Russia)		Palearctic	
Clarification	Average for all samples ± standard deviation	Standard Error of the Mean	95% confidence interval lower values	95% confidence interval upper values						
Indicator	A ± s, µm	SE Mean, µm	95.0 % CI lower values, µm	95.0 % CI upper values, µm	Min, µm	Max, µm	Min, µm	Max, µm	Min, µm	Max, µm
Seminal vesicula length*	69.99±4.063	0.742	68.534	71.442	N/M	N/M	N/M	N/M	N/M	N/M
Seminal vesicula width*	55.48±2.394	0.437	54.624	56.338	N/M	N/M	N/M	N/M	N/M	N/M
Excretory vesicula length*	156.77±1.243	0.227	156.328	157.217	N/M	N/M	N/M	N/M	N/M	N/M
Excretory vesicula weight*	47.22±3.117	0.569	46.108	48.339	N/M	N/M	N/M	N/M	N/M	N/M
Excretory bladder length*	60.76±1.504	0.275	60.219	61.296	N/M	N/M	N/M	N/M	N/M	N/M
Excretory bladder width*	18.83±1.338	0.244	18.354	19.312	N/M	N/M	N/M	N/M	N/M	N/M
Excretory pore length*	10.81±1.009	0.184	10.444	11.166	N/M	N/M	N/M	N/M	N/M	N/M
Excretory pore width*	10.50±1.031	0.188	10.128	10.865	N/M	N/M	N/M	N/M	N/M	N/M

Data from	Present study				Gherasim et al., 2016		Chikhlyaev et al., 2012		Skrjabin, 1970	
Host	*Pelophylax esculentus* complex, *Rana temporaria*				*Rana ridibunda, R. lessonae* and *R.esculenta*		*R. esculenta*		*R. arvalis, R. dalmatina, R.esculenta, R. ridibunda, R. temporara, R.tigrina, Bufo calamita, B. variabilis, B. viridis, B.vulgaris, Bombina variegata, Hyla arborea*	
Country	Latvia				Moldova		Midde Volga region (Russia)		Palearctic	
Clarification	Average for all samples ± standard deviation	Standard Error of the Mean	95% confidence interval lower values	95% confidence interval upper values						
Indicator	A ± s, µm	SE Mean, µm	95.0 % CI lower values, µm	95.0 % CI upper values, µm	Min, µm	Max, µm	Min, µm	Max, µm	Min, µm	Max, µm
Spine length (anterior region)*	8.61±0.187	0.034	8.540	8.674	N/M	N/M	N/M	N/M	N/M	N/M
Spine width (anterior region)*	1.96±0.122	0.022	1.920	2.008	N/M	N/M	N/M	N/M	N/M	N/M
Spine length (lateral surface)*	12.40±0.528	0.096	12.215	12.593	N/M	N/M	N/M	N/M	N/M	N/M
Spine width (lateral surface)*	1.468±0.017	0.003	1.669	1.682	N/M	N/M	N/M	N/M	N/M	N/M
Spine length (posterior part)*	15.23±0.904	0.165	14.905	15.552	N/M	N/M	N/M	N/M	N/M	N/M
Spine width (posterior part)*	1.88±0.030	0.005	1.867	1.888	N/M	N/M	N/M	N/M	N/M	N/M
Spine length (region of excretory pore)*	13.89±0.586	0.107	13.679	14.098	N/M	N/M	N/M	N/M	N/M	N/M
Spine width (region of excretory pore)*	1.46±0.038	0.007	1.450	1.477	N/M	N/M	N/M	N/M	N/M	N/M

Data from	Present study				Gherasim et al., 2016		Chikhlyaev et al., 2012		Skrjabin, 1970	
Host	*Pelophylax esculentus* complex, *Rana temporaria*				*Rana ridibunda, R. lessonae* and *R.esculenta*		*R. esculenta*		*R. arvalis, R. dalmatina, R.esculenta, R. ridibunda, R. temporara, R.tigrina, Bufo calamita, B. variabilis, B. viridis, B.vulgaris, Bombina variegata, Hyla arborea*	
Country	Latvia				Moldova		Midde Volga region (Russia)		Palearctic	
Clarification	Average for all samples ± standard deviation	Standard Error of the Mean	95% confidence interval lower values	95% confidence interval upper values						
Indicator	A ± s, µm	SE Mean, µm	95.0 % CI lower values, µm	95.0 % CI upper values, µm	Min, µm	Max, µm	Min, µm	Max, µm	Min, µm	Max, µm
Distance between spines in anterior part of the body*	2.73±0.230	0.042	2.647	2.812	N/M	N/M	N/M	N/M	N/M	N/M
Distance between spines in posterior part of the body*	4.34±0.455	0.083	4.173	4.498	N/M	N/M	N/M	N/M	N/M	N/M
Distance between spines in end of the body*	4.39±0.129	0.024	4.339	4.431	N/M	N/M	N/M	N/M	N/M	N/M
Egg length	26.48±0.749	0.137	26.209	26.745	11	18	11	15	22	34
Egg width	13.76±0.349	0.064	13.635	13.885	18	12	19	25	11	17

* - original data

N/M – not measured

All measures in current study performed after sample staining with benzanthrone luminophore